# Dynein-ADP as a Force-Generating Intermediate Revealed by a Rapid Reactivation of Flagellar Axoneme

Tomomi Tani and Shinji Kamimura
Department of Biology, Graduate College of Arts and Sciences, University of Tokyo, Komaba, Meguro-ku 3–8-1, Tokyo 153-8902, Japan

ABSTRACT Fragmented flagellar axonemes of sand dollar spermatozoa were reactivated by rapid photolysis of caged ATP. After a time lag of 10 ms, axonemes treated with protease started sliding disintegration. Axonemes without protease digestion started nanometer-scale high-frequency oscillation after a similar time lag. Force development in the sliding disintegration was measured with a flexible glass needle and its time course was corresponded well to that of the dynein-ADP intermediate production estimated using kinetic rates previously reported. However, with a high concentration (~80 $\mu$M) of vanadate, which binds to the dynein-ADP intermediate and forms a stable complex of dynein-ADP-vanadate, the time course of force development in sliding disintegration was not affected at all. In the case of high frequency oscillation, the time lag to start the oscillation, the initial amplitude, and the initial frequency were not affected by vanadate, though the oscillation once started was damped more quickly at higher concentrations of vanadate. These results suggest that during the initial turnover of ATP hydrolysis, force generation of dynein is not blocked by vanadate. A vanadate-insensitive dynein-ADP is postulated as a force-generating intermediate.

## INTRODUCTION

The movement of flagella is coupled with ATP turnover by the axonemal dynein. The relationship between the beat frequency of reactivated flagella and ATP concentration shows a good fit to the Michaelis-Menten equation (Brokaw and Benedict, 1968; Gibbons and Gibbons, 1972). Based on the model for the actin-myosin system (Lymn and Taylor, 1971), the pre-steady state kinetics of ATP turnover by *Tetrahymena* outer dynein has been analyzed (Johnson, 1983; Porter and Johnson, 1983; Holzbaur and Johnson, 1989a,b). It has been revealed that ATP binds to dynein and is hydrolyzed rapidly. Release of the products (phosphate and ADP) is relatively slow, with the release of ADP being the rate-limiting step. Because the acceleration of this step occurs on rebinding of dynein to microtubules (Omoto and Johnson, 1986), the dynein-ADP intermediate is assumed to be related to the interaction with microtubules and force generation. However, little evidence has been reported about the direct relationship between the force generation and intermediate states within the ATPase cycle, mainly because of the difficulties in measuring the force generation by dynein.

When fragmented flagellar axonemes are treated with protease, they show sliding disintegration after the application of MgATP (Summers and Gibbons, 1971). Fragmented flagellar axonemes without proteolytic digestion do not slide or bend, but show oscillatory sliding along the length of the axonemes with amplitudes of several nanometers and with frequencies of ~300 Hz in the presence of ATP (Kamimura and Kamiya, 1989, 1992).

We describe here experiments regarding the kinetics of force generation on the sliding disintegration and the high frequency oscillation in fragmented flagellar axonemes after a rapid photolysis of caged ATP. We also examine the kinetics in the presence of vanadate, a potent inhibitor of dynein (Kobayashi et al., 1978; Gibbons et al., 1978) that forms a stable complex with the dynein-ADP intermediate after phosphate is released from the dynein-ADP-$P_i$ (Shimizu, 1981; Shimizu and Johnson, 1983). From the rate of force generation and inhibition by vanadate after the photolysis of caged ATP, we infer which intermediate of dynein ATPase is responsible for the force generation.

## MATERIALS AND METHODS

### Preparation of demembranated sperm flagella

Spermatozoa from the sand dollar, *Clypeaster japonicus* or *Scaphechinus mirabilis*, were demembranated as described by Gibbons et al. (1982), with some modifications. Dry sperm taken from the sand dollar were suspended in 10 volumes of filtered natural sea water. The suspension was mixed with 10 volumes of extracting solution containing 0.04% (w/v) Triton X-100, 0.2 M potassium acetate, 2 mM $MgCl_2$, 0.5 mM EGTA, 0.1 mM EDTA, 2 mM dithiothreitol (DTT), and 10 mM Tris-HCl (pH 8.0). The mixture was gently swirled for 30–60 s at room temperature (25°C). After extraction, the suspension of demembranated sperm axonemes was diluted in 10 volumes of reactivation solution containing 0.2 M potassium acetate, 2 mM $MgCl_2$, 0.5 mM EGTA, 0.1 mM EDTA, 4 mM DTT, and 40 mM Hepes-KOH (pH 8.0). The suspension was transferred into an homogenizer with a Teflon pestle tube and subjected to 10–15 strokes to fragment the flagellar axonemes into 5- to 20-$\mu$m lengths. The fragmented axonemes were then introduced into a flow chamber. The flow chamber was made by putting a square frame made of stainless steel (5 × 5 × 1 mm) between two pieces of coverslip treated with 3-aminopropyltriethoxysilane (Shin-Etsu, Tokyo). After 5 min, the chamber was perfused with reactivation solution

*Received for publication 7 July 1998 and in final form 4 June 1999.*

Dr. Tani's present address: Pacific Biomedical Research Center, University of Hawaii, Snyder 306, 2538 The Mall, Honolulu, HI 96822. E-mail: tani@pbrc.hawaii.edu.

Address reprint requests to Shinji Kamimura, Department of Biology, Graduate College of Arts and Sciences, University of Tokyo, Komaba, Meguro-ku, Tokyo 153-8902, Japan. Tel.: 81-3-5454-6665; Fax: 81-3-5454-6998; E-mail: kam@nano.c.u-tokyo.ac.jp.



0006-3495/99/09/1518/10 $2.00

to wash out floating fragments. For the experiments to observe sliding disintegration, axonemes fixed on coverslips were pre-treated with 10 $\mu$g ml$^{-1}$ elastase (Type III, Sigma Chemical, St. Louis, MO) in the reactivation solution for 2.5–3.0 min at room temperature (25°C). Finally, the reactivation solution containing caged ATP (lot: CL002, Dojindo, Kumamoto) and 20 $\mu$g ml$^{-1}$ apyrase (grade VII, Sigma) was introduced into the chamber. Apyrase was used to remove contaminating ATP and/or ADP derived from caged ATP solution. All the experiments were carried out at room temperature (25°C).

## Force measurements

Forces exerted by axonemes were measured as described in previous reports (Yoneda, 1960; Kamimura and Takahashi, 1981; Oiwa and Takahashi, 1988) with some modifications and improvements. A glass needle was made by attaching the end of a glass rod to a heated platinum wire and pulling the melted glass out from the wire. After treating with 3-aminopropyltriethoxysilane, the glass needle (tip diameter, 0.5–1.0 $\mu$m; length, ~50 $\mu$m) was introduced into the chamber using a micromanipulator (*ULTRA* line, Newport Corp., Irvine, CA) so that the tip of the glass needle was attached to an axoneme at a right angle. The elastic coefficient of each needle was measured by cross-calibration with a needle of known elastic coefficient (Yoneda, 1960). The needles with elastic coefficients of 0.5–20 pN nm$^{-1}$ were chosen for the experiments. Mechanical compliance between the axonemes and the glass surfaces (needles and chambers) was negligible in our experiments because of the tight adhesion due to the aminopropyl-silane coating.

## Optical components

Fig. 1 is a schematic diagram of the experimental setup. A 100W mercury arc lamp (UI-100, Ushio Electric, Tokyo) was used as a source of ultraviolet light for the photolysis of caged ATP. An electromagnetic shutter (No. 0 model, Copal, Tokyo) and filters (U-330 and UV-300, HOYA Optics, Tokyo) were placed between the arc lamp and a dichroic mirror (Asahi Spectra Co., Tokyo). Through the objective lens (D-Apo UV 100×, Olympus, Tokyo), the axonemes were irradiated with ultraviolet light under Koehler illumination conditions. The irradiated area was approximately 150 $\mu$m in diameter. The electromagnetic shutter was open for 10 ms. The percentage of photolysed caged ATP present in the solution after one ultraviolet light pulse was estimated from the beat frequency of reactivated flagellar axonemes to be approximately 50%. Images of fragmented axoneme and the glass needle were observed under the bright field illumination from a 50W tungsten-halogen lamp. To reduce the ultraviolet light from the tungsten-halogen lamp, sharp cut filters (SC 50, FUJI Photo Film Corp., Tokyo) were placed in the light path between the lamp and the condenser.

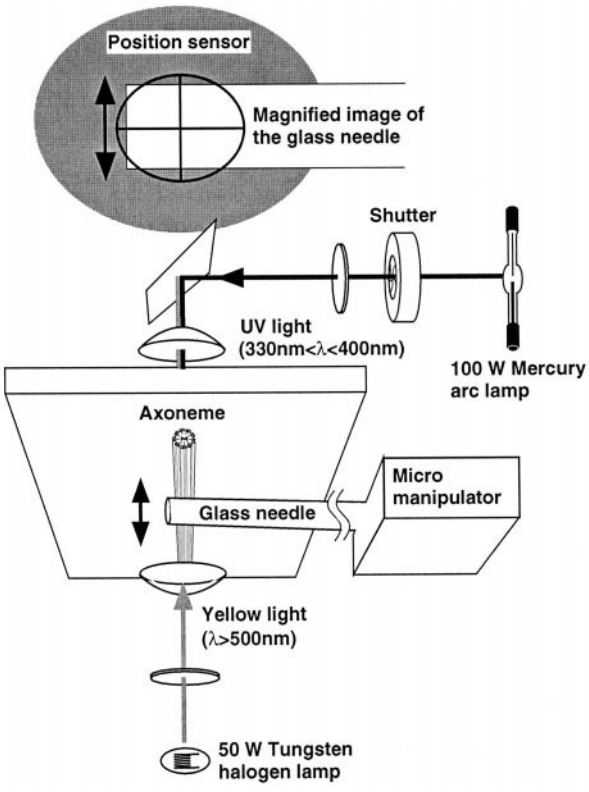


FIGURE 1 A schematic diagram of the experimental system. See text for further details.

The bright field image of the needle's tip was focused onto a quadrant photo detector (S 1557, Hamamatsu Photonics Co., Hamamatsu, Japan). The photo-sensing area was 1 mm in diameter. The final magnification of the image was 560×. The intensity of light coming into each divided area was measured with current-voltage converters (OPA-111, Burr-Brown, Tucson, AZ) with feedback resistors of 2 G ohm. The range of measurable displacement was <500 nm, depending on both the diameter of the glass needle and the intensity of illumination. By using the apparatus described above, the displacement of the needle along the axonemal axis was measured with a spatial and temporal resolution of better than 1 nm and 1 kHz, respectively (Kamimura, 1987). The output signal of the needle displacement was recorded on MO disks through an A-D converter (Canopus Electronics, Kobe, Japan) in a personal computer (9801-FX, NEC, Tokyo) with a sampling rate of 20 kHz. Calibrations of the needle displacement and the photosensor output were carried out after each experiment as follows. The position of the photosensor was displaced in the direction perpendicular to the needle axis by a micrometer (MHM, Mitsutoyo, Tokyo) and the output voltage of the photosensor was measured. The displacement of the sensor corresponding to the output of 1V was divided by the magnification of the microscope image to obtain the final relationship between the displacement of the glass needle and the sensor output. Typically, a 1 V sensor output was obtained per 10–50 nm displacement.

## Estimation of photo-released ATP concentration in the reactivation solution

The time course of ATP release from caged ATP was inferred from the rate of the characteristic transmission change of 406 nm light (McCray et al., 1980), as described previously (Tani and Kamimura, 1998). The ATP concentration was expected to exceed a threshold level for the reactivation of motility within a few ms, and reached 90% of the maximal concentration (approximately 1 mM) in 100 ms when a reactivation solution with 2 mM caged ATP was used.

# RESULTS

## Force development during sliding disintegration after the photolysis of caged ATP

Using flagellar axonemes digested with elastase, the time course of force generation during sliding disintegration after the rapid application of ATP was examined. When an axoneme in the reactivation solution containing 0.2 M potassium acetate, 2 mM $MgCl_2$, 0.5 mM EGTA, 0.1 mM EDTA, 4 mM dithiothreitol (DTT), 40 mM Hepes-KOH (pH 8.0), 20 $\mu$g ml$^{-1}$ apyrase, and 2 mM caged ATP was irradiated with ultraviolet light (wavelength, 330–400 nm) for 10 ms, the tip of the attached needle was observed to be displaced along with the sliding disintegration of the axoneme after a

time lag of approximately 10 ms from the beginning of the ultraviolet light pulse. A typical example of the needle's displacement is shown in Fig. 2A. The motion of the needle ceased within 50–60 ms when the maximal force exerted by the axoneme was assumed to be balanced by the elastic force produced by the glass needle. The maximal displacement of the needle (20–200 nm) varied with each trial, presumably depending on both the length of fragmented axoneme (5–20 $\mu$m) and the elastic coefficient of the glass needle used (0.5–20 pN nm$^{-1}$). However, the time course of the displacement was almost the same in each case. The maximal forces measured were within a range of 100–250 pN.

All the data obtained were normalized so that the maximal force developed was equal to 1.0. The averaged time course of force development was then compared with the estimated population change of dynein in each intermediate (dynein-ATP, dynein-ADP-$P_i$ and dynein-ADP) after the photolysis of caged ATP (Fig. 2 *B*). Because there have been no reported kinetic rate constants of ATP turnover in sea urchin/sand dollar axonemal dynein, we employed those of purified *Tetrahymena* 22S dynein ATPase (dynein outer arm) that were reported by Johnson and coworkers (Holzbaur and Johnson, 1989a), although we realize that the rates could be somewhat different from those of echinoderm dynein. The time course of photolytic release of ATP in our optical setup and acceleration of ADP release in the presence of microtubules (Omoto and Johnson, 1986; Shimizu et al., 1989; Holzbaur and Johnson, 1989b) were also taken into account. Differential equations involving [dynein-ATP], [dynein-ADP-$P_i$] and [dynein-ADP] were solved by using *Mathematica* 3.0 (Wolfram Research Inc., Champaign, Illinois).

As shown in Fig. 2 *B*, the estimated time course of the increase of the dynein-ADP intermediate closely fits the averaged time course of force development. This is the first demonstration of the pre-steady state transient of force generation by dyneins in situ.

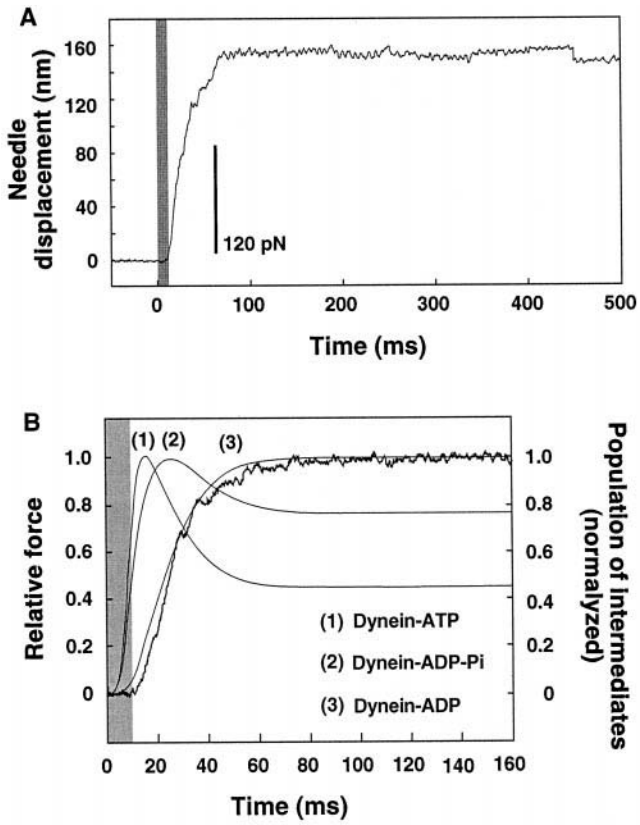


FIGURE 2 *A*: Time courses of force development measured with a glass needle with an elastic coefficient, 1.2 pN nm$^{-1}$. Shaded part indicates the time when 10 ms-ultraviolet light pulse was applied. *B*: Time course of averaged force development in sliding disintegration and the simulated time course of the production of dynein ATPase intermediates. An averaged time course of seven independent sets of data measured on different axonemes with different glass needles (elastic coefficients of 0.5–20 pN nm$^{-1}$) is shown. Simulated time courses of increase in the normalized population of dynein-ATP (1), dynein-ADP-$P_i$ (2) and dynein ADP (3) are superimposed on the same figure. The rate constants for ATP binding, $k_{+1} = 4\ s^{-1}\ \mu M^{-1}$ and $k_{-1} = 0.15\ s^{-1}$; for ATP hydrolysis, $k_{+2} = 50\ s^{-1}$ and $k_{-2} = 3\ s^{-1}$; phosphate release, $k_{+3} = 70\ s^{-1}$ and $k_{-3} = 8000\ s^{-1}\ M^{-1}$; ADP release, $k_{+4} = 40\ s^{-1}$ and $k_{-4} = 0.015\ s^{-1}\ \mu M^{-1}$ (Holzbaur and Johnson 1989a; Omoto and Johnson, 1986) were used for the calculation. *Shaded part* indicates the time when 10 ms ultraviolet light pulse was given. All the curves were normalized by adjusting the maximum value to 1.0.

## High frequency oscillation after the photolysis of caged ATP

When the fragmented axonemes had not been digested by elastase, nm-scale high frequency oscillation of the axoneme was observed (Kamimura and Kamiya, 1989, 1992) after the photolysis of 2 mM caged ATP. Concomitantly with the start of oscillation (amplitude, ~5 nm), in many cases, displacements of the glass needle in one direction of up to 50 nm (a, in Fig. 3) were observed. Such motion was

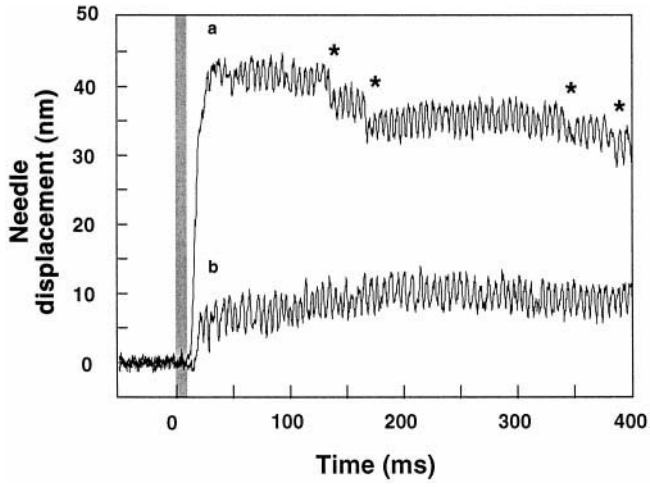


FIGURE 3 Starting transient of high-frequency oscillation after the photolysis of 2 mM caged ATP. Typical examples of displacement after the first (*a*) and second (*b*) applications of ATP in the same axoneme measured by the same glass needle are shown. *Shaded part* indicates the time when 10 ms ultraviolet light pulse was applied. Asterisks indicate the stepwise shifts of the center line during the oscillation.

observed only on the first application of ATP and became smaller or was not observed at all with the following application of ATP (b, in Fig. 3). The direction of the displacement, if any, was the same in the repeated experiments using the same axoneme. In some cases, the center line of the oscillation shifted in a stepwise manner as indicated by asterisks in Fig. 3.

As in the time course of force development during sliding disintegration (Fig. 2, *A* and *B*), the onset of high frequency oscillation had a time lag of approximately 10–15 ms (Fig. 4 *A*). The amplitude (Fig. 4 *B*) reached a maximum (4.8 ± 0.9 nm) within 20 ms, which was constant throughout the oscillation, and did not vary with the length of fragmented axonemes (5–20 $\mu$m) or the elastic coefficient of the glass needle used for the measurements. This indicates that the major factor determining the amplitude of this oscillation is not the elasticity of the glass needle, but the internal structure of the axoneme. The frequency of oscillation exceeded 200 Hz within 20 ms of the ultraviolet light pulses (Fig. 4 *C*). The frequency gradually decreased after it reached a maximum, possibly due to the depletion of ATP either by diffusion or by hydrolytic activity of dynein and/or apyrase.

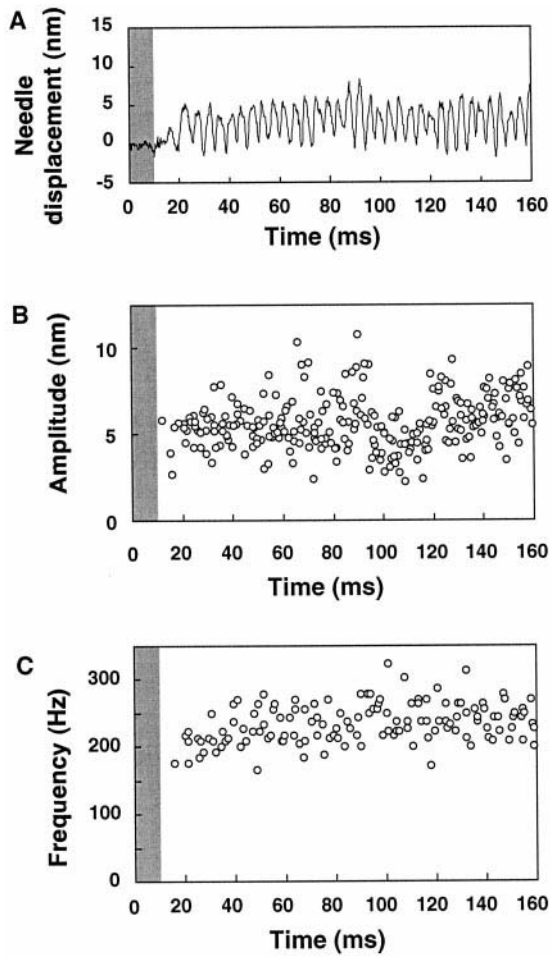


FIGURE 4 *A*: A typical example showing a transient of the oscillation frequency after the photolysis of 2 mM caged ATP. *B*: Time course of change in the amplitude of oscillation. The peak-to-peak distance is measured and plotted against the time after the beginning of ultraviolet light pulse. Results of four measurements obtained from the same axoneme are superimposed on the same figure. *C*: Time course of change in the frequency of oscillation, the inverse of the peak-to-peak period of the oscillation, is plotted against time. Results of four measurements obtained from the same axoneme are superimposed. *Shaded part* indicates the time when 10 ms ultraviolet light pulse was applied.

## Effects of vanadate on high frequency oscillation after the photolysis of caged ATP

For a more detailed investigation of the intermediate of dynein, which is important for the force generation, the effect of vanadate on the starting transient of high-frequency oscillation was examined. Vanadate is a potent inhibitor of dynein that is assumed to act as a phosphate analogue and bind to the dynein-ADP intermediate (Shimizu, 1981; Shimizu and Johnson, 1983).

Fragmented axonemes were pre-incubated in the reactivation solution containing 2 mM caged ATP, 20–80 $\mu$M vanadate, and 80 $\mu$g ml$^{-1}$ apyrase. Starting transients of the oscillation in axonemes after the photolysis of caged ATP in the presence and absence of vanadate are shown in Fig. 5 (*A*, without vanadate; *B*, 20 $\mu$M vanadate; *C*, 80 $\mu$M vanadate). The axoneme started oscillation within 10–15 ms from the beginning of the ultraviolet light pulse at a frequency as high as 200 Hz, independently of the concentration of vanadate we examined. The timing of the initiation of oscillation was essentially the same irrespective of the presence (Fig. 5, *B* and *C*) or absence (Fig. 5 *A*) of vanadate. However, vanadate finally quenched the motion under the experimental condition, that is, axonemes completely ceased oscillation within 100–150 ms when the concentration of vanadate in the solution was 80 $\mu$M (Fig. 5 *C*). In the solution containing apyrase, activity of the oscillation was recovered within 1–2 min, and the same experiment could be repeated using the same axoneme. The duration of oscillation tended to be shortened gradually after repeated trials for unknown reasons. Therefore, only the data of the first or second measurement of each axoneme was used for further analyses.

As in the case of the oscillation amplitude, the time course of the frequency change showed that vanadate had little effect on the starting transient of oscillation (Fig. 5 *D*, without vanadate; Fig. 5 *E*, 20 $\mu$M vanadate; Fig. 5 *F*, 80 $\mu$M vanadate). Although oscillation ceased earlier with a higher concentration of vanadate, the initial oscillation frequencies were almost the same, independent of the concentration of vanadate. In the presence of a lower concentration of vanadate (20 $\mu$M), the frequency of oscillation gradually decreased (Fig. 5 *E*), with prolonged intervals between successive downward displacements (Fig. 6 *A*). However, the amplitude and the maximal sliding velocity (calculated from the maximal slope of displacement, ~7 $\mu$m s$^{-1}$) were almost constant until the oscillation stopped completely (Fig. 6 *B*).

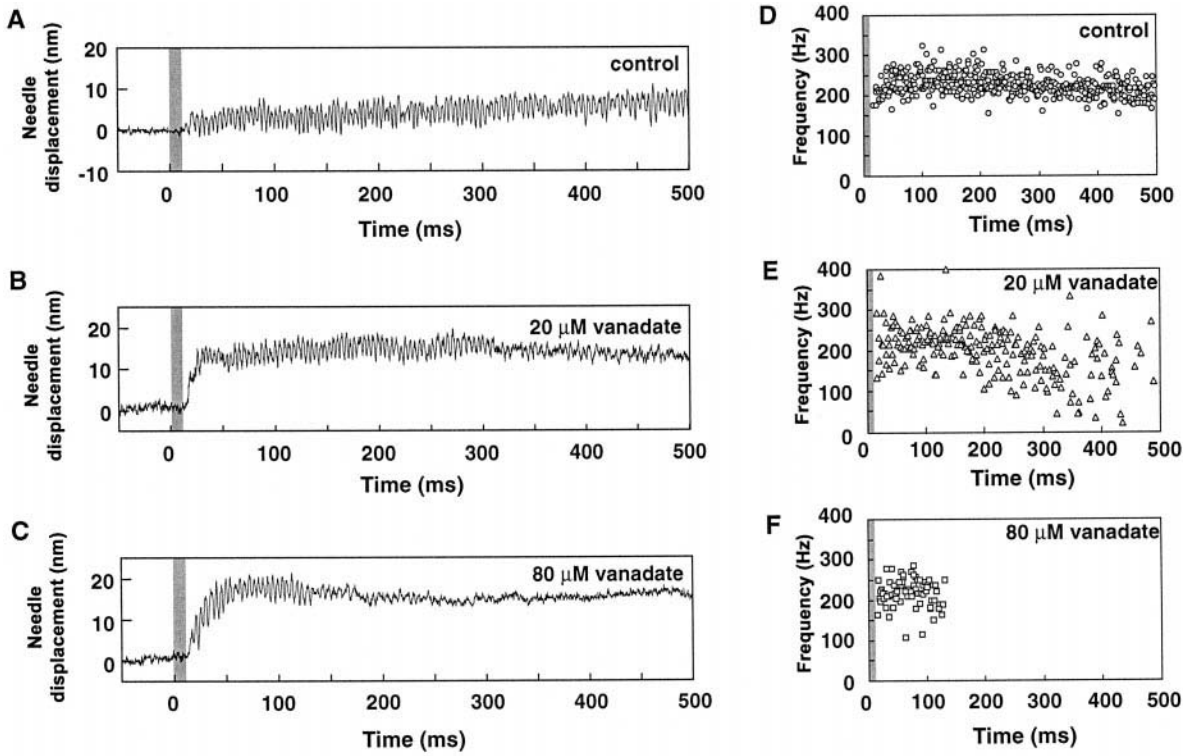


FIGURE 5 Effects of vanadate on the nm-scale oscillation of fragmented axonemes. *A-C*: starting transients of oscillation in a solution without vanadate (*A*), with 20 $\mu$M vanadate (*B*) and 80 $\mu$M vanadate (*C*) after a rapid reactivation by the photolysis of 2 mM caged ATP. The initial displacements of needles as stated in Fig. 3 were observed. *D-F*: time courses of change in the frequency of oscillation in a solution without vanadate (*D*), with 20 $\mu$M vanadate (*E*) or 80 $\mu$M vanadate (*F*) after the photolysis of caged ATP (data from four different axonemes were plotted against the time after the ultraviolet light pulses). *Shaded part* indicates the time when 10 ms ultraviolet light pulse was applied.

### Effects of vanadate on the force development during sliding disintegration after the photolysis of caged ATP

Digested axonemes in a reactivation solution containing 2 mM caged ATP and 80 $\mu$M vanadate were irradiated with ultraviolet light for 10 ms. As observed in the absence of vanadate, the tip of the needle started to move simultaneously with the sliding disintegration of the axoneme after a time lag of approximately 10 ms from the beginning of the ultraviolet light pulse. It ceased to move within 60 ms, which was similar to the time course observed without vanadate. A typical example is shown in Fig. 7 *A*. The maximal forces measured were within a range of 40–140 pN. As in the case of high frequency oscillation, the activity was recovered completely within 1–2 min in the solution containing apyrase and the same experiment could be repeated using the same axoneme.

To compare the time courses of force development with and without vanadate, averaged and normalized data in both experiments are shown in Fig. 7 *B*. Except for a short delay ($\sim$10 ms) shown in the presence of vanadate, both time courses were observed to be similar. This result indicates that the initial transient of force generation after the rapid application of ATP is affected little by the presence of 80 $\mu$M vanadate.

Strangely, although dynein activities were assumed to be completely blocked in $\sim$150 ms when exposed to 80 $\mu$M vanadate (Fig. 5, *C* and *F*), no backward recovery motion of the glass needles was observed in many cases ($\sim$ 70%) after they ceased to move at the point that the forces were balanced.

## DISCUSSION

### Dynein-ADP as a force-producing intermediate

Caged ATP was used to examine the time course of force generation by axonemal dynein in situ, and the relationship between the ATPase cycle and the force generation of dynein was investigated. In the case of sliding disintegration, the time course of force development after the photolysis of caged ATP fits well with that of the increase of the computer-estimated dynein-ADP intermediate. This estimate was based on the rate constants of 22S dynein ATPase activity determined by Johnson and coworkers (Holzbaur and Johnson, 1989a), with an assumption of a 10-fold acceleration of the ADP release (from 4 $s^{-1}$ to 40 $s^{-1}$) by microtubules (Omoto and Johnson, 1986). Provided that the force produced by axonemes is proportional to the number of force-generating dynein molecules in the axoneme, this result can be regarded as the first direct evidence that dynein

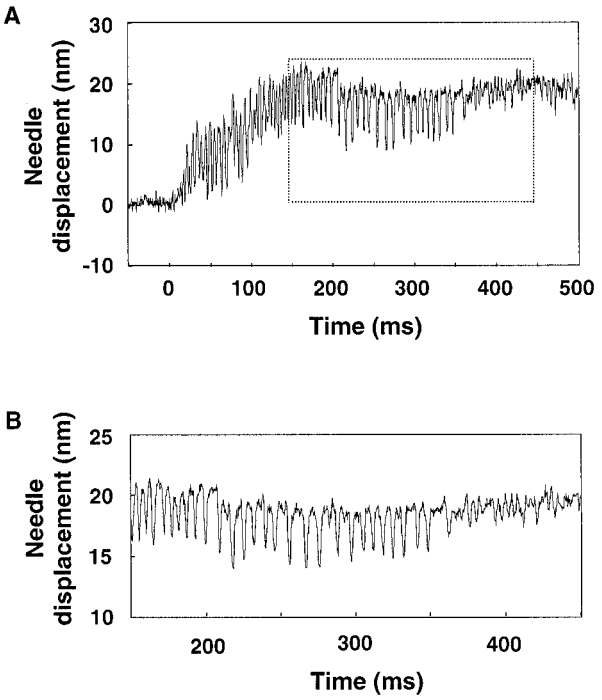


FIGURE 6 The inhibitory effects of vanadate on high frequency oscillation. *A*: High-frequency oscillation reactivated by the photolysis of 2 mM caged ATP in the presence of 20 $\mu$M vanadate. *B*: Detail of the transient of vanadate inhibition which corresponds to the area indicated by the *dotted rectangle* in *A*.

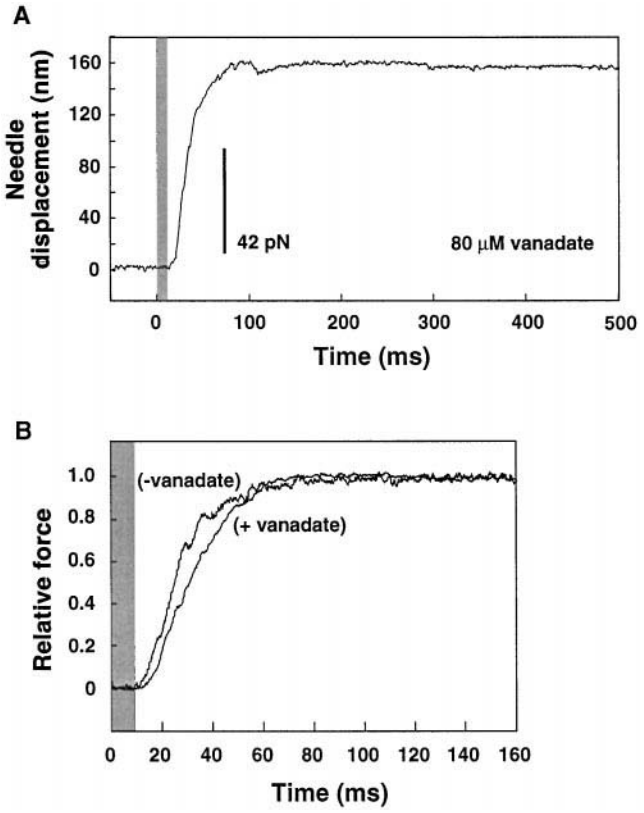


FIGURE 7 *A*: Time course of force development during sliding disintegration after the photolysis of 2 mM caged ATP in the presence of 80 $\mu$M vanadate. A glass needle with elastic coefficient of 0.42 pN nm$^{-1}$ was used. *Shaded part* indicates the time when 10 ms ultraviolet light pulse was given. *B*: Comparison of the time course of averaged force development in sliding disintegration between with (+vanadate) and without (−vanadate) vanadate (80 $\mu$M). Twelve sets of data (+vanadate) and seven sets of data (−vanadate) were used for the averaging. *Shaded part* indicates the time when 10 ms ultraviolet light pulse was applied.

generates the sliding force while it is in the state of a dynein-ADP intermediate.

Caged ATP has been used for many studies of chemomechanical coupling of motor proteins, especially for actin-myosin systems (McCray et al., 1980; Goldman et al., 1982; Hibberd et al., 1985). However, it is also known to work as a competitive inhibitor in an actin-myosin system (Thirlwell et al., 1995) and a microtubule-kinesin system (Higuchi et al., 1997). In the case of axonemal dynein, caged ATP was shown to lower the beat frequency of reactivated flagella, and the estimated Ki was 1.0–1.4 mM (Tani and Kamimura, 1998). Even if caged ATP competes with ATP to bind to dynein with a similar binding constant, it would cause further delay of as short as 5 ms in the estimated increase of the dynein-ADP intermediate. It should be noted that the increase of the dynein-ADP-$P_i$ intermediate could not be fitted to the increase of force production with any arbitrary rate constants of caged ATP binding and ADP release.

Another possibility that can lead to an incorrect simulation is if inner dynein arms, which have different motile and enzymatic activities from outer dynein, are involved in the initial onset of motility after ATP application. However, from the velocity analyses of microtubule sliding in high-salt treated axonemes of sea-urchin spermatozoa (Yano and Miki-Noumura, 1980) and in *Chlamydomonas* mutants (Kagami and Kamiya, 1992; Yagi et al., 1994), it has been suggested that the sliding activity observed in intact axonemes mainly depends on the outer dynein arms. These reports explain why we have assumed that outer dyneins are mainly responsible for the production of sliding forces in elastase-treated echinoderm sperm axonemes.

One of the most characteristic features of the $\beta$ heavy chain of outer dynein is that it has four nucleotide-binding sites (Gibbons et al., 1991; Ogawa, 1991). Under our experimental conditions ATP/ADP concentration was kept very low with the presence of 20 $\mu$g/ml apyrase (260 units mg$^{-1}$). In these conditions, all the binding sites were assumed to be free from nucleotides, and such a state could affect the binding affinity of the catalytic nucleotide-binding site. However, apyrase ranging from 20 to 400 $\mu$g/ml did not cause any significant effects on the onset of sliding disintegration. Because we have no positive evidence of any physiological significance for non-catalytic binding sites for ATP, further detailed analyses will be required. Experiments using fluorescent ATP analogues (Inaba et al., 1989; Omoto, 1992; Mocz et al., 1998) might provide us with more insight into this problem.

In our series of experiments, we used echinoderm sperm flagella instead of *Tetrahymena* cilia, which had been pre-

viously used for the kinetics studies. Using echinoderm sperm flagella in our experiments provided several advantages. First, there are several reports of physiological studies on the velocity and force production during sliding disintegration (Kamimura and Takahashi, 1981; Takahashi et al., 1982; Oiwa and Takahashi, 1988). In addition, after treating with elastase, microtubule sliding is known to occur mostly between only two sets of doublet bundles (Shingyoji and Takahashi, 1995). In the case of reactivated *Tetrahymena* cilia, on the contrary, "piggy-backing." which is thought to be caused by multiple sliding among the nine doublets, can often be observed after protease treatment, which makes the results of force production more complicated.

## Nanometer-scale high frequency oscillation reflects the activity of a small fraction of dynein

We examined a starting transient of nanometer-scale high frequency oscillation in the axoneme after the photolysis of caged ATP. The oscillation started after a time lag (~10 ms) similar to that shown in the case of sliding disintegration. However, the time courses for the amplitude and frequency to reach plateaus were as fast as 20 ms, which were far faster than those of the force development during sliding disintegration and the estimated increase in the dynein-ADP intermediate. This indicated that each back-and-forth shear motion of the oscillation would not be the result of the synchronized behavior of thousands of dynein arms contained in one fragmented axoneme and that each oscillatory motion could be executed by a relatively small fraction of dynein arms. It is most likely that the amplitude of oscillation reflects the unitary distance of motion, and the frequency reflects the intrinsic rates of dynein attachment/detachment to microtubules.

The large displacement of the needle by up to 50 nm along with the initiation of oscillatory motion was an interesting but unexpected phenomenon, since the fragmented axoneme should never disintegrate without protease treatment and the amplitudes of steady-state oscillation are restricted to within several nanometers (Kamimura and Kamiya, 1989). However, such a large displacement in axonemes would not be unreasonable, because doublet microtubules in intact flagella were actually shown to slide out each other with amplitudes larger than 100 nm during beating (Brokaw, 1989) as is also expected from bend angles (Gibbons, 1982). When demembranated sea urchin sperm flagellar axonemes with rigor waves (Gibbons and Gibbons, 1974) are reactivated by rapid photolysis of caged ATP, flagella resume bending movements as if they had been beating in steady state without any pause (Tani and Kamimura, 1998). It might be possible to assume that a certain switching mechanism which controls tubule sliding up to ~100 nm depends on the waveforms, and could still be working even after the rigor axonemes are fragmented (a, in Fig. 3). Such a switching mechanism may be reset once the axonemes are reactivated with ATP (b, in Fig. 3).

## Onset of force generation by dynein is not affected by the presence of vanadate

The effects of vanadate on the onset of high frequency oscillation of fragmented axonemes were examined. It was revealed that the amplitude, the length of time lag before the onset and the initial frequency were not affected by the presence of vanadate in the range of 20–80 $\mu$M (Fig. 5). The oscillation decayed in a concentration-dependent manner, i.e., the motion ceased in 300–500 ms at 20 $\mu$M vanadate and ~150 ms at 80 $\mu$M vanadate. It should be noted that during inhibition, frequency of oscillation decreased without a change in amplitude or in maximal sliding velocity. The oscillations only became less regular, with longer and more variable intervals between their downward spikes (Fig. 6). This observation supports the idea that each back-and-forth oscillation reflects the activity of different sets of a small number of dynein arms being activated in turn, which is blocked by vanadate in an almost all-or-nothing manner.

In addition, we investigated the effects of vanadate on the force production during the sliding disintegration of protease-treated axonemes. Pre-incubation with 80 $\mu$M vanadate had little effect on the time course of force development (Fig. 7). This indicates that during the initial starting transients, the force generation by dynein is not blocked by vanadate.

## Two different kinds of dynein-ADP intermediates are involved in the ATPase cycle

On the bases of the data described above, we simulated the change in the population of active dynein in the presence of vanadate. Although no quantitative measurement of the rate of association of vanadate to dynein has been reported, the rate is estimated to be faster by a factor of $10^6$ than that for the corresponding steps with myosin (Goodno and Taylor, 1982; Shimizu and Johnson, 1983), and the second-order rate constant of vanadate binding to the dynein-ADP intermediate was thought to be within a range of $10^5$–$10^7$ $s^{-1}$ $M^{-1}$ (Shimizu, personal communication). The kinetic scheme of vanadate inhibition is shown by the following scheme, which was reported by Shimizu and Johnson (1983):

$$\text{Dynein-ADP-Pi} \underset{k_{-3}}{\overset{k_{+3}}{\rightleftharpoons}} \text{Dynein-ADP} \underset{k_{-4}}{\overset{k_{+4}}{\rightleftharpoons}} \text{Dynein}$$

$$k_{-\mathrm{v}} \Uparrow\Downarrow k_{+\mathrm{v}}$$

Dynein-ADP-Vanadate

(Scheme I)

By employing the simulation as shown in Fig. 2 *B*, the inhibition constant of vanadate to dynein (10 nM, Shimizu, 1981) and the possible second-order rate constant of vanadate binding to the dynein-ADP ($k_{+\mathrm{v}}$) (from $10^4$ $s^{-1}$ $M^{-1}$ to

$10^7$ $s^{-1}$ $M^{-1}$), we calculated how the population of the dynein-ADP intermediate was lowered in the presence of vanadate (Fig. 8, *A* and *B*). If the rate of binding is as low as $10^4$ $s^{-1}$ $M^{-1}$, the decrease in the population of dynein-ADP is too slow to change the rate of production of dynein-ADP and, in the case of 80 $\mu$M vanadate, more than 80% of dynein is estimated to still be active even after 500 ms from the photolysis of caged ATP (Fig. 8 *B*). This seems to be consistent with our observation that the rate of force production during sliding disintegration was not lowered by vanadate (Fig. 7). However, obviously this can not be the case since the high frequency oscillation was shown to be blocked within ~150 ms at 80 $\mu$M vanadate (Fig. 5 *C*).

If the rate of binding is as high as $10^6$ $s^{-1}$ $M^{-1}$, the production of dynein-ADP is completely blocked within 200 ms after the application of ATP, which shows good coincidence with the time course of inhibition of oscillation as shown in Fig. 5 *C*. However, this leads to another question of why the time course of force production during sliding disintegration was not altered by vanadate, since the production of the dynein-ADP intermediate is expected to be greatly reduced to less than 25% of that without vanadate and the plateau of the production comes within 40 ms (Fig. 8 *B*), which is far faster than that of force production during sliding disintegration.

Therefore, we postulate that there are at least two different states of the dynein-ADP intermediate with different binding affinities to vanadate (Scheme II) and that force production occurs at the state of dynein-ADP that has a low affinity to vanadate, dynein-$ADP_{(1)}$, before it turns into the intermediate that has a high affinity to vanadate, dynein-$ADP_{(2)}$. A similar kinetics scheme with two different dynein-ADP states was also suggested by biochemical studies (Holzbaur and Johnson, 1989a,b).

$$\text{Dynein-ADP-Pi} \underset{k_{-3}}{\overset{k_{+3}}{\rightleftharpoons}} \text{Dynein-ADP}_{(1)} \underset{k_{-f}}{\overset{k_{+f}}{\rightleftharpoons}} \text{Dynein-ADP}_{(2)} \underset{k_{-4}}{\overset{k_{+4}}{\rightleftharpoons}} \text{Dynein}$$

$$k_{-v} \Uparrow\Downarrow k_{+v}$$

$$\text{Dynein-ADP}_{(2)}\text{-Vanadate}$$

(Scheme II)

In this scheme we assumed that dynein-$ADP_{(2)}$, which is a state with high binding affinity to vanadate, would be produced after the conformational change of dynein accompanied with force generation. Preliminary simulation on the basis of Scheme II showed that the concentration change of dynein-$ADP_{(1)}$ fitted better than that simulated based on Scheme I if we chose the rate of transition from dynein-$ADP_{(1)}$ to dynein-$ADP_{(2)}$ ($k_{+f}$) as 20–40 $s^{-1}$ and the rate of binding between vanadate and dynein-$ADP_{(2)}$ to be $10^6$ $s^{-1}$ $M^{-1}$.

So far, several possibilities have been discussed about the force-generating intermediate of dynein. Many ultrastructural studies have revealed a difference between the conformations of dynein with and without ATP, especially in the presence of vanadate (Witman and Minervini, 1982; Goodenough and Heuser, 1982; Tsukita et al., 1983; Burgess, 1995). From the kinetic analysis of the dynein ATPase pathway, a change in conformation is thought to occur during the dynein-ADP state (Holzbaur and Johnson, 1989a).

Based on the analyses of proteolytic digestion, Inaba and Mohri (1989) assumed that the dynein-ADP-$P_i$ intermediate is in a state with a conformation which is different from nucleotide-free dynein. They discussed the idea that the conformational change involving force generation occurred at the state of the dynein-ADP-$P_i$ intermediate, because the conformation of the dynein-ADP-vanadate complex had been assumed to mimic that of the dynein-ADP-$P_i$ intermediate (Shimizu and Johnson, 1983). However, from our present results, it is more likely that this conformational change occurs with the transition from dynein-$ADP_{(1)}$ to dynein-$ADP_{(2)}$ which is thought to correspond to the step of force generation.

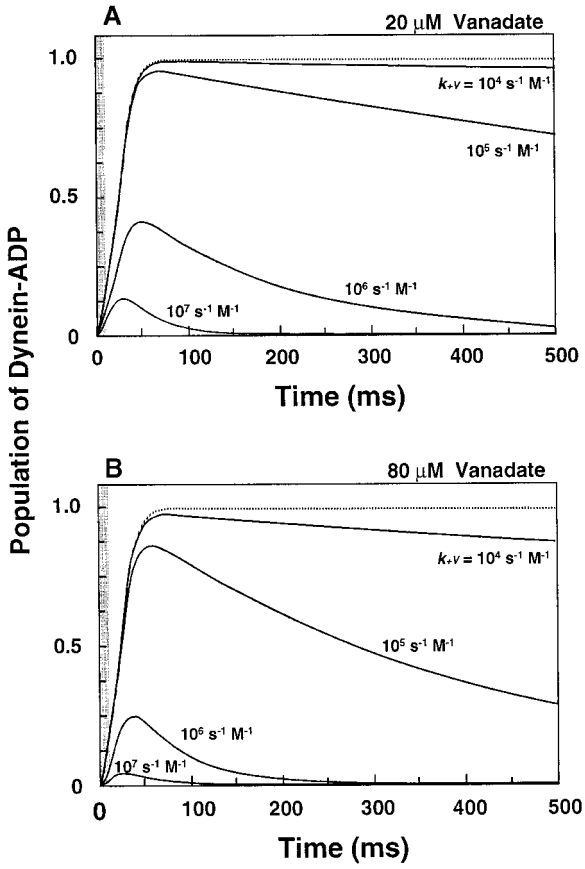


FIGURE 8 Simulated time course of [dynein-ADP] in the presence of 20 $\mu$M vanadate *(A)* and 80 $\mu$M vanadate *(B)*. The second-order rate constant of vanadate binding to dynein-ADP ($k_{+v}$) ranged from $10^4$ $s^{-1}$ $M^{-1}$ to $10^7$ $s^{-1}$ $M^{-1}$, and an inhibition constant of 10 nM (Shimizu, 1981) were used for the simulation. Other rate constants used are the same as those in Fig. 2 *B*. *Dotted lines* represent the cases in the absence of vanadate.

### Cross-links between dynein-ADP-vanadate complex and microtubules

The dynein-ADP-vanadate complex has been shown to be in weakly bound to microtubules. For example, Sale and Gibbons (1979) observed that trypsin-treated flagellar axonemes immersed in a solution containing vanadate were split into a few groups of curved doublet microtubules instead of showing linear sliding disintegration after the addition of MgATP. Okuno (1980) showed that the stiffness of axonemes incubated with vanadate and ADP was 15-fold lower than that of rigor axonemes. Microtubules on a glass slide covered with purified 22S dynein showed Brownian motion predominantly along the length of microtubule in the presence of vanadate and ATP (Vale et al., 1989).

However, the result obtained in our experiments was inconsistent with these observations. In most cases, in the presence of vanadate and ATP, once doublet tubules showed active sliding, they did not return to their original position by the elastic force of the glass needles even after force generation was thought to be completely blocked (Fig. 7, *A* and *B*). So far we do not have a plausible explanation for this ratchet-like behavior of sliding in the axoneme. It might be possible that some of the inner dynein heavy chains form rigor-like cross-links to microtubules at the state of enzyme-ADP-vanadate complex.

The combination of caged ATP with vanadate is a unique experimental system to reveal the relationship between the ATPase cycle and the motility of dyneins because the association/dissociation rates of vanadate with axonemal dynein are expected to be far faster than those with myosin (Goodno and Taylor, 1982) and presumably with kinesin (Vale et al., 1985). This combination is useful for the identification of active sites along the axonemes in beating flagella and cilia, as well as the kinetic study of force generation in a single dynein molecule.

We thank Drs. T. Shimizu, R. A. Thornhill, and R. D. Allen for critically reading the manuscript and Drs. R. Kamiya and C. K. Omoto for useful advice and discussion. This work was supported by a grant-in-aid for scientific research from the Ministry of Education of Japan.

## REFERENCES

Brokaw, C. J. 1989. Direct measurements of sliding between outer doublet microtubules in swimming sperm flagella. *Science.* 243:1593–1596.

Brokaw, C. J., and B. Benedict. 1968. Mechanochemical coupling in flagella. I. Movement-dependent dephosphorylation of ATP in glycerinated spermatozoa. *Arch. Biochem. Biophys.* 125:770–778.

Burgess, S. A. 1995. Rigor and relaxed outer dynein arms in replicas of cryofixed motile flagella. *J. Mol. Biol.* 250:52–63.

Gibbons, I. R. 1982. Sliding and bending in sea urchin sperm flagella. *In* Symp. Soc. Exp. Biol. vol. 35, Prokaryotic and Eukaryotic Flagella. W. B. Amos and J. G. Duckette, eds. Cambridge University Press, Cambridge. 225–287.

Gibbons, B. H., and I. R. Gibbons. 1972. Flagellar movement and adenosine triphosphatase activity in sea-urchin sperm extracted with Triton X-100. *J. Cell Biol.* 54:78–97.

Gibbons, B. H., and I. R. Gibbons. 1974. Properties of flagellar "rigor waves" formed by abrupt removal of adenosine triphosphate from actively swimming sea urchin sperm. *J. Cell Biol.* 63:970–985.

Gibbons, I. R., M. K. Cosson, J. A. Evans, B. H. Gibbons, B. Houck, K. H. Martinson, W. S. Sale, and W-J. Y Tang. 1978. Potent inhibition of dynein adenosine triphosphatase and of the motility of cilia and sperm flagella by vanadate. *Proc. Natl. Acad. Sci. USA.* 75:2220–2224.

Gibbons, I. R., J. A. Evans, and B. H. Gibbons. 1982. Acetate anions stabilize the latency of dynein 1 ATPase and increase the velocity of tubule sliding in reactivated sperm flagella. *Cell Motil. (suppl.)* 1:181–184.

Gibbons, I. R., B. H. Gibbons, G. Mocz, and D. J. Asai. 1991. Multiple nucleotide-binding sites in the sequence of dynein $\beta$ heavy chain. *Nature.* 352:640–643.

Goldman, Y. E., M. G. Hibberd, J. A. McCray, and D. R. Trentham. 1982. Relaxation of muscle fibres by photolysis of caged ATP. *Nature.* 300: 701–705.

Goodenough, U. W., and J. E. Heuser. 1982. Substructure of the outer dynein arm. *J. Cell Biol.* 95:798–815.

Goodno, C. C., and E. W. Taylor. 1982. Inhibition of myosin ATPase by vanadate. *Proc. Natl. Acad. Sci. USA.* 79:21–25.

Hibberd, M. G., J. A. Dantzig, D. R. Trentham, and Y. E. Goldman. 1985. Phosphate release and force generation in skeletal muscle fibers. *Science.* 228:1317–1319.

Higuchi, H., E. Muto, Y. Inoue, and T. Yanagida. 1997. Kinetics of force generation by single kinesin molecules activated by laser photolysis of caged ATP. *Proc. Natl. Acad. Sci. USA.* 94:4395–4400.

Holzbaur, E. L., and K. A. Johnson. 1989a. ADP release is rate limiting in steady-state turnover by the dynein adenosinetriphosphatase. *Biochemistry.* 28:5577–5585.

Holzbaur, E. L., and K. A. Johnson. 1989b. Microtubules accelerate ADP release by dynein. *Biochemistry.* 28:7010–7016.

Inaba, K., M. Okuno, and H. Mohri. 1989. Anthraniloyl ATP, a fluorescent analog of ATP, as a substrate for dynein ATPase and flagellar motility. *Arch. Biochem. Biophys.* 274:209–215.

Inaba, K., and H. Mohri. 1989. Dynamic conformational changes of 21S dynein ATPase coupled with ATP hydrolysis revealed by proteolytic digestion. *J. Biol. Chem.* 264:8384–8388.

Johnson, K. A. 1983. The pathway of ATP hydrolysis by dynein: kinetics of a presteady state phosphate burst. *J. Biol. Chem.* 258:13825–13832.

Kagami, O., and R. Kamiya. 1992. Translocation and rotation of microtubules caused by multiple species of Chlamydomonas inner-arm dynein. *J. Cell Sci.* 103:653–664.

Kamimura, S. 1987. Direct measurement of nanometric displacement under an optical microscope. *Applied Optics.* 26:3425–3427.

Kamimura, S., and K. Takahashi. 1981. Direct measurement of the force of microtubule sliding in flagella. *Nature.* 293:566–568.

Kamimura, S., and R. Kamiya. 1989. High-frequency nanometre-scale vibration in 'quiescent' flagellar axonemes. *Nature.* 340:476–478.

Kamimura, S., and R. Kamiya. 1992. High-frequency vibration in flagellar axonemes with amplitudes reflect the size of tubulin. *J. Cell Biol.* 116:1443–1454.

Kaplan, J. H., B. Forbush, III, and J. H. Hoffman. 1978. Rapid photolytic release of adenosine 5′-triphosphate from a protected analogue: Utilization by the Na: K pump of human red blood cell ghosts. *Biochemistry.* 17:1929–1935.

Kobayashi, T., T. Martensen, J. Nath, and M. Flavin. 1978. Inhibition of dynein ATPase by vanadate and its possible use as a probe for the role of dynein in cytoplasmic motility. *Biochem. Biophys. Acta.* 16:146–154.

Lymn, R. W., and E. W. Taylor. 1971. Mechanism of adenosine triphosphate hydrolysis by actomyosin. *Biochemistry.* 10:4617–4624.

McCray, J. A., L. Herbette, T. Kihara, and D. R. Trentham. 1980. A new approach to time-resolved studies of ATP-requiring biological systems: laser flash photolysis of caged ATP. *Proc. Natl. Acad. Sci. USA.* 77: 7237–7241.

Mocz, G., M. K. Helms, D. M. Jameson, and I. R. Gibbons. 1998. Probing the nucleotide binding sites of axonemal dynein with the fluorescent

nucleotide analogue 2′(3′)-O-(-N-Methylanthraniloyl)-adenosine 5′-triphosphate. *Biochemistry.* 37:9862–9869.

Ogawa, K. 1991. Four ATP-binding sites in the midregion of the β heavy chain of dynein. *Nature.* 352:643–645.

Oiwa, K., and K. Takahashi. 1988. The force-velocity relationship for microtubule sliding in demembranated sperm flagella of sea urchin sperm. *Cell Struct. Func.* 13:193–205.

Okuno, M. 1980. Inhibition and relaxation of sea urchin sperm flagella by vanadate. *J. Cell Biol.* 85:712–725.

Omoto, C. K. 1992. Sea urchin sperm axonemal motion supported by fluorescent, ribose-modified analogues of ATP. *J. Musc. Res. Cell Motil.* 13:635–639.

Omoto, C. K., and K. A. Johnson. 1986. Activation of the dynein adenosine triphosphatase by microtubules. *Biochemistry.* 25:419–427.

Porter, M. E., and K. A. Johnson. 1983. Transient state kinetic analysis of the ATP-induced dissociation of the dynein-microtubule complex. *J. Biol. Chem.* 258:6582–6587.

Sale, W. S., and I. R. Gibbons. 1979. Study of the mechanism of vanadate inhibition of the dynein cross-bridge cycle in sea urchin sperm flagella. *J. Cell Biol.* 82:291–298.

Shimizu, T. 1981. Steady-state kinetic study of vanadate-induced inhibition of ciliary dynein adenosinetriphosphatase activity from *Tetrahymena. Biochemistry.* 20:4347–4354.

Shimizu, T., and K. A. Johnson. 1983. Presteady state kinetic analysis of vanadate-induced inhibition of the dynein ATPase. *J. Biol. Chem.* 258: 13833–13840.

Shimizu, T., S.-P. Marchese-Rogana, and K. A. Johnson. 1989. Activation of the dynein adenosine triphosphatase by cross-linking to microtubules. *Biochemistry.* 28:7016–7021.

Shingyoji, C., and K. Takahashi. 1995. Cyclical bending movements induced locally by successive iontophoretic application of ATP to an elastase-treated flagellar axoneme. *J. Cell Sci.* 108:1359–1369.

Summers, K. E., and I. R. Gibbons. 1971. Adenosine triphosphate-induced sliding of tubules in trypsin-treated flagella of sea-urchin sperm. *Proc. Natl. Acad. Sci. USA.* 68:3092–3096.

Takahashi, K., C. Shingyoji, and S. Kamimura. 1982. Microtubule sliding in reactivated flagella. In Symp. Soc. Exp. Biol. vol. 35, Prokaryotic and Eukaryotic Flagella. W. B. Amos and J. G. Duckette, eds. Cambridge University Press, Cambridge. 159–177.

Tani, T., and S. Kamimura. 1998. Reactivation of sea-urchin sperm flagella induced by rapid photolysis of caged ATP. *J. Exp. Biol.* 201:1493–1503.

Thirlwell, H., J. A. Sleep, and M. A. Ferenczi. 1995. Inhibition of unloaded shortening velocity in permeabilized muscle fibres by caged ATP compounds. *J. Muscle Res. Cell Motil.* 16:131–137.

Tsukita, S., S. Tuskita, J. Usukura, and H. Ishikawa. 1983. ATP-dependent changes of the outer dynein arm in *Tetrahymena* cilia: a freeze-etch replica study. *J. Cell Biol.* 96:1480–1485.

Vale, R. D., B. J. Schnapp, T. Mitchison, E. Steuer, T. S. Reese, and M. P. Sheetz. 1985. Different axoplasmic proteins generate movement in opposite directions along microtubules in vitro. *Cell.* 43:623–632.

Vale, R. D., D. R. Soll, and I. R. Gibbons. 1989. One dimensional diffusion of microtubules bound to flagellar dynein. *Cell.* 59:915–925.

Witman, G. B., and N. Minervini. 1982. Dynein arm conformation and mechanochemical transduction in the eukaryotic flagellum. Prokaryotic and eukaryotic flagella. W. B. Amos and J. G. Duckette, eds. Cambridge University Press, Cambridge. 203–223.

Yagi, T., S. Kamimura, and Y. Kamiya. 1994. Nanometer scale vibration in mutant axonemes of *Chlamydomonas. Cell Motil. Cytoskeleton.* 29: 177–185.

Yano, Y., and Miki-Noumura 1980. Sliding velocity between outer doublet microtubules of sea-urchin sperm axonemes. *J. Cell Sci.* 44:169–186.

Yoneda, M. 1960. Force exerted by a single cilium of *Mytilus edulis*. *Int. J. Exp. Biol.* 37:461–468.